Supporting information

Ultrathin Ni-MOF nanosheet arrays grown on polyaniline decorated Ni foam as an advanced electrode for asymmetric supercapacitor with high energy density

Qiuhui Cheng,[a] Kai Tao,[a,b*] Xue Han,[a] Yujing Yang,[a] Zheng Yang,[a] Qingxiang Ma[b] and Lei Han[a*]

[a] School of Materials Science & Chemical Engineering, Ningbo University, Ningbo, Zhejiang 315211, China

E-mail: taokai@nbu.edu.cn (K. Tao), hanlei@nbu.edu.cn (L. H.)

[b] State Key Laboratory of High-Efficiency Coal Utilization and Green Chemical Engineering, Ningxia University, Yinchuan 750021, China

Experimental section

Materials: 1, 4-benzenedicarboxylic acid (terephthalic acid, H_2BDC, $C_8H_6O_4$, 98.0%) was purchased from TCI Chemicals. $NiCl_2 \cdot 6H_2O$ (99.5%), Aniline (99%), ammonium persulfate ($(NH_4)_2S_2O_8$, APS, 98.0%), hydrochloric acid (HCl, 36.0~38.0%), N,N-dimethylformamide (DMF, 99.8 %) and ethanol (99 %) were purchased from Sinopharm Chemical Reagent Co., Ltd. All the solvents and reagents were of analytical grade and used without further purification. Deionized water was obtained from local sources. Ni foam (NF) was cleaned thoroughly with ethanol and H_2O in an ultrasonic bath and then dried at 80 ^oC.

Preparation of PANI/NF: A piece of pretreated NF (1 cm×1 cm) was immersed into 20 mL HCl solution (1 M) containing 54.7 μL aniline. Then, another 20 mL HCl solution (1 M) containing 0.0685 g APS was dropwise added to the above solution, and the in situ polymerization of aniline to polyaniline (PANI) was performed in an ice bath below 5 ^oC for 10 h. Finally, PANI modified Ni foam (PANI/NF) was taken out, and then rinsed with copious deionized water followed by drying at 60 ^oC in an oven.

Preparation of Ni-MOF/PANI/NF: Typically, 0.237 g $NiCl_2 \cdot 6H_2O$ and 0.166 g H_2BDC were dissolved in 35 mL DMF under magnetic stirring to a homogenous solution, and then 2.5 mL ethanol and 2.5 mL deionized water were added. The mixture was further stirred for 30 min. After that, a piece of PANI/NF was soaked in the mixture, and the mixture containing PANI/NF was transferred into a Teflon-lined autoclave. The autoclave was kept in an oven at 125 ^oC for 12 h. After cooling to

room temperature, the Ni-MOF deposited PANI/NF (Ni-MOF/PANI/NF) was obtained, and then rinsed with copious deionized water followed by drying at 60 ^{o}C in an oven.

Preparation of Ni-MOF/NF: The Ni-MOF/NF is prepared by the same synthetic procedure as that of Ni-MOF/PANI/NF except for replacing PANI/NF support with NF. The Ni-MOF powder was collected from the bottom of the autoclave, and then washed with copious deionized water followed by drying at 60 ^{o}C.

Preparation of Ni-MOF powder electrode: The Ni-MOF powder electrode was prepared by mixing Ni-MOF powder (80 wt%), polyvinylidene fluoride (10 wt%) and acetylene black (10 wt%) with a few drops of ethanol to form a slurry, and then was casted onto NF. The as prepared electrode was dried at 70 °C overnight and pressed at 10 MPa. The loading density of Ni-MOF powder was about 1.8 mg/cm^2.

Characterization: X-ray diffraction (XRD) patterns were collected from a Bruker AXS D8 Advance X-ray diffractometer with Cu Kαradiation (1.5406 Å, 40 kV, 40 mA). Scanning electron microscopy (SEM) images and energy dispersive X-ray spectroscopy (EDS) spectra were obtained from a Hitachi S-4800 field emission scanning electron microscope (FESEM). Transmission electron microscopy (TEM) and high resolution TEM (HRTEM) images, selected area electron diffraction (SAED) pattern, and elemental mapping were acquired on an FEI Tecnai TF20 transmission electron microscope operated at 200 kV. X-ray photoelectron spectroscopy (XPS) measurement was performed on a Thermo Scientific ESCA-Lab-200i-XL spectrometer (Waltham, MA).

Electrochemical measurements: Electrochemical measurements were carried out in three-electrode cell using 2 M KOH as electrolyte solution. The active materials deposited NF, saturated calomel electrode (SCE) and platinum foil electrode were used as the working electrode, reference electrode and counter electrode, respectively. The asymmetric supercapacitor (ASC) was assembled using Ni-MOF/PANI/NF as positive electrode and activated carbon (AC) electrode as negative electrode in 2 M KOH. The AC electrode was prepared by the same method as Ni-MOF powder electrode. The loading density of AC was about 7.48 mg/cm^2. The electrochemical performances of electrodes were evaluated by cyclic voltammetry (CV), galvanostatic charge-discharge (GCD) and electrochemical impedance spectroscopy (EIS) with an electrochemical workstation (CHI 660E, Chenhua Shang, China). The areal capacitance (C_s) was determined from discharge curves based on following equation:

$$C_s = \frac{I\Delta t}{S\Delta V} \quad (1)$$

Where I, Δt, ΔV, and S are the discharge current, discharge time, voltage window and area of the electrode, respectively.

The energy density (E, W h kg^{-1}) and power density (P, W kg^{-1}) of the ASC device were determined by following formulas:

$$E = \frac{C_S(\Delta V)^2}{2 \times 3.6} \quad (2)$$

$$P = \frac{3600 \times E}{\Delta t} \quad (3)$$

Where Cs (F g^{-1}), ΔV (V), and Δt (s) are the specific capacitance, potential window, and discharge time, respectively.

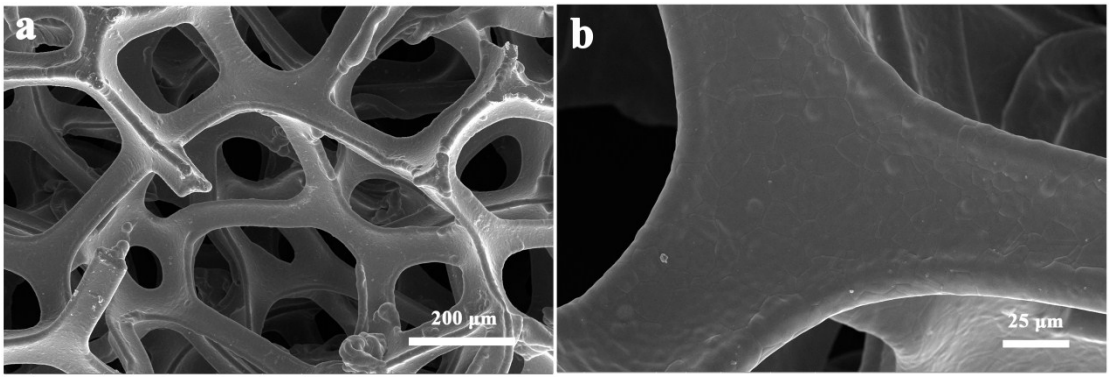

Fig. S1 (a,b) SEM images of bare Ni foam at different magnifications.

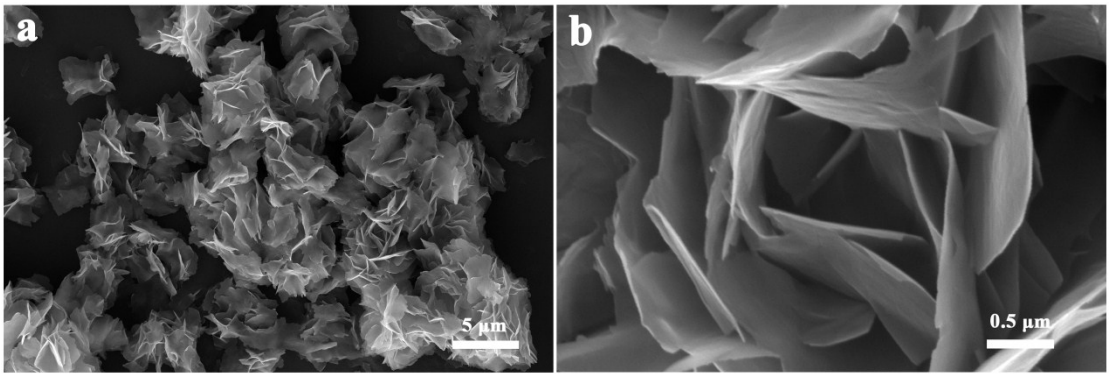

Fig. S2 (a,b) SEM images of Ni-MOF powder at different magnifications.

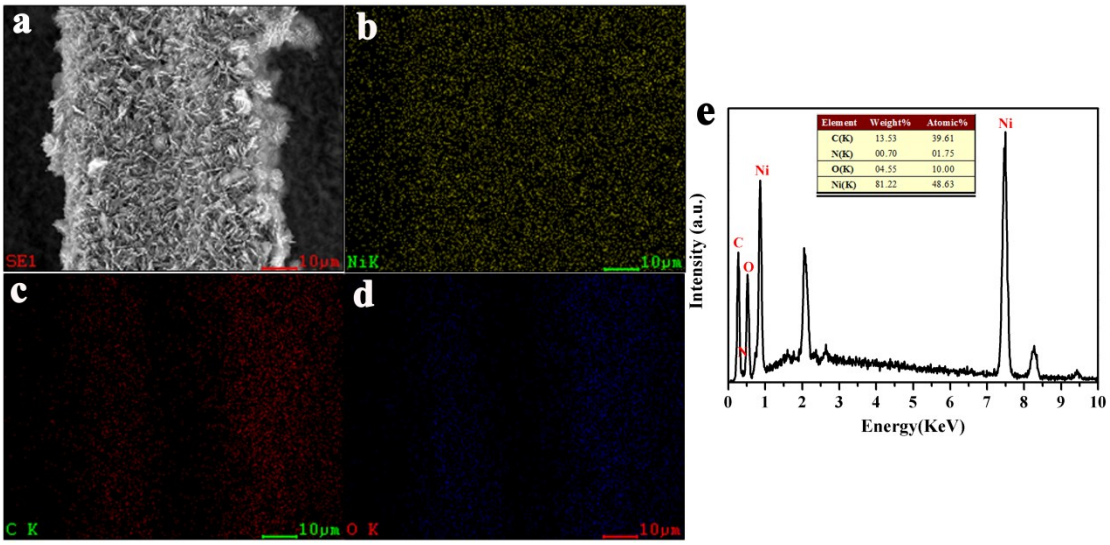

Fig. S3 (a-d) SEM image and elemental mappings of Ni-MOF/PANI/NF. (e) Energy dispersive X-ray spectroscopy (EDS) elemental analysis of Ni-MOF/PANI/NF.

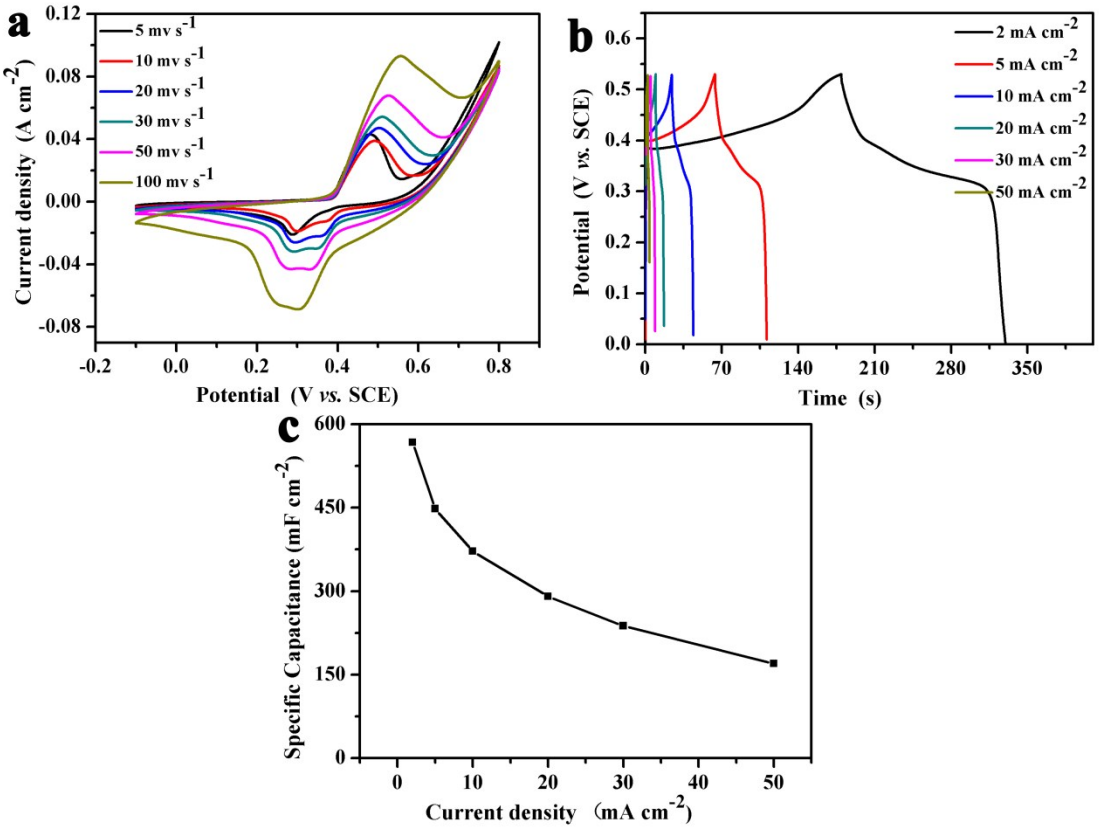

Fig. S4 (a) CV curves of Ni-MOF powder at the scan rate of 5-100 mV s^{-1}. (b) GCD curves of Ni-MOF powder at the current density of 2-50 mA cm^{-2}.

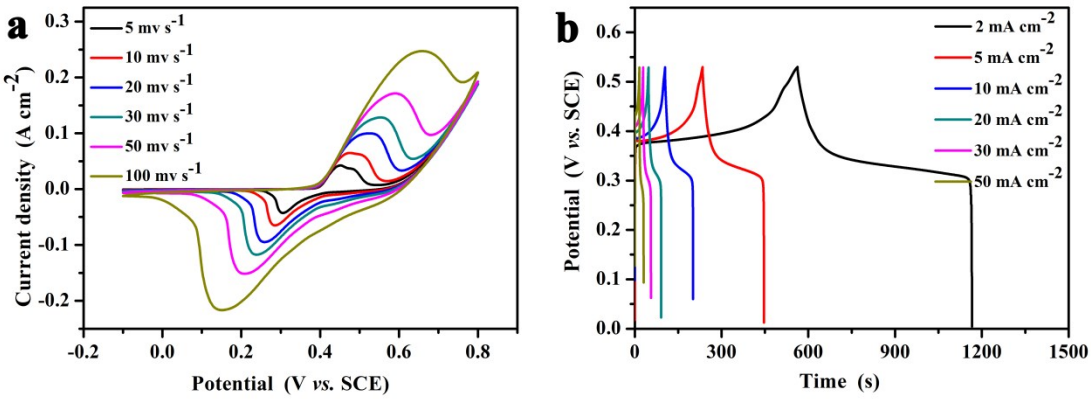

Fig. S5 (a) CV curves of Ni-MOF/NF at the scan rate of 5-100 mV s^{-1}. (b) GCD curves of Ni-MOF/NF at the current density of 2-50 mA cm^{-2}.

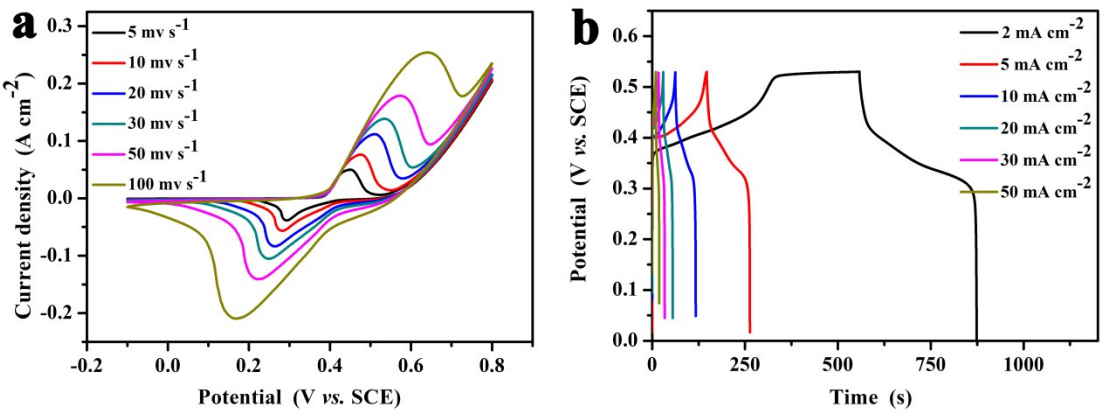

Fig. S6 (a) CV curves of PANI/NF at the scan rate of 5-100 mV s^{-1}. (b) GCD curves of PANI/NF at the current density of 2-50 mA cm^{-2}.

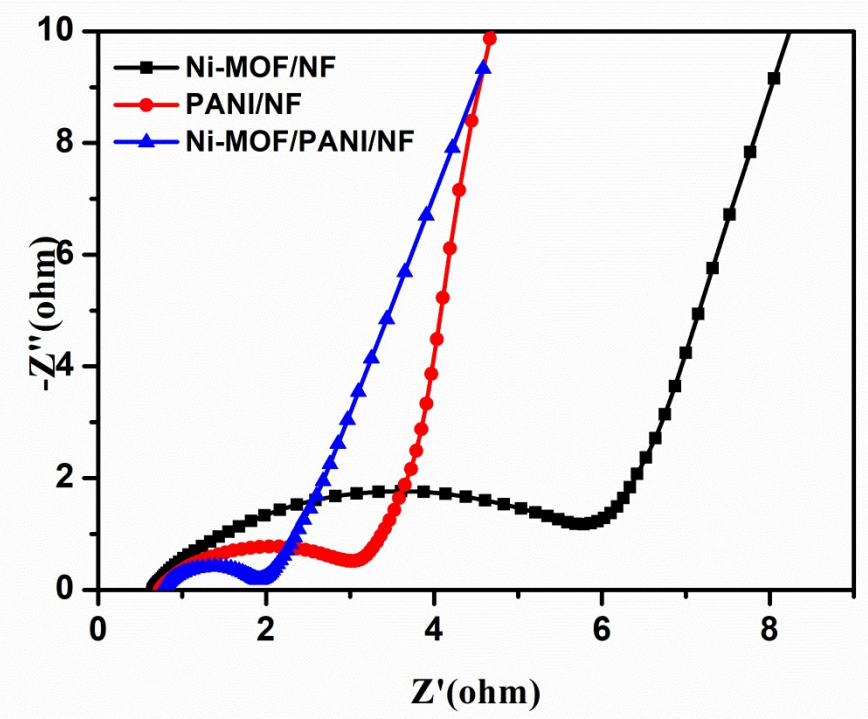

Fig. S7 Nyquist plots of Ni-MOF/NF, PANI/NF and Ni-MOF/PANI/NF electrodes.

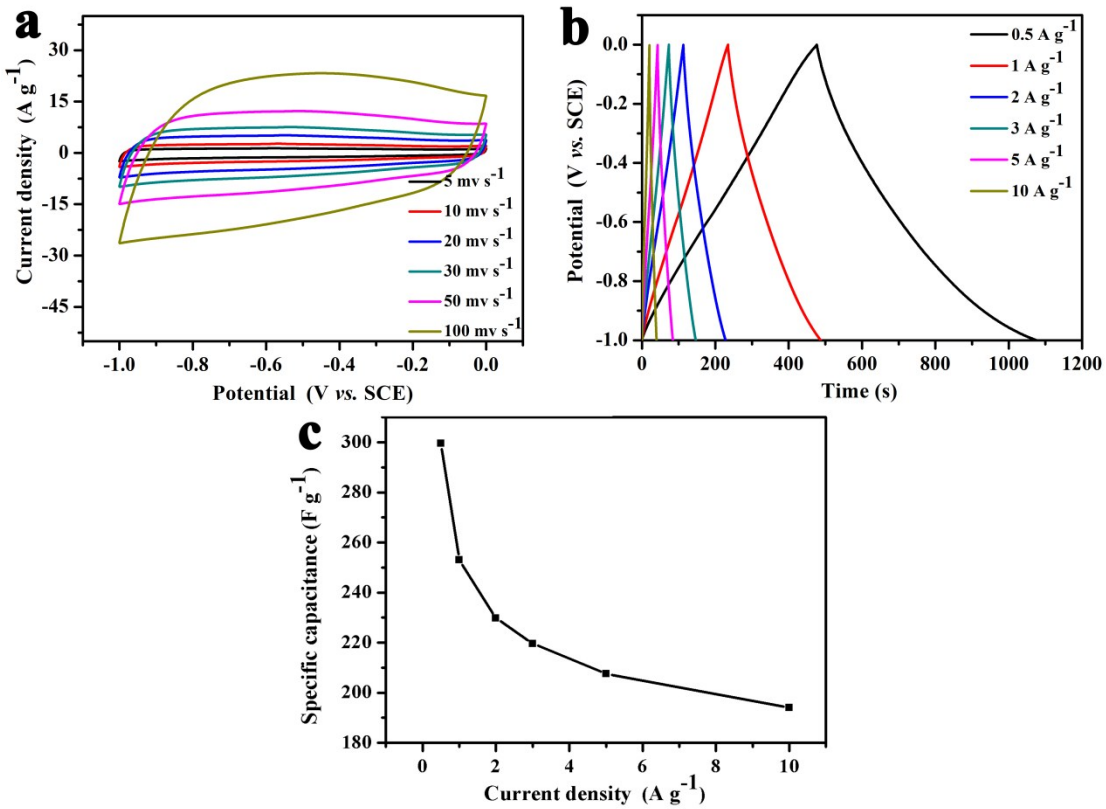

Fig. S8 (a) CV curves of AC electrode at different scan rates, (b) GCD curves of AC electrode at different current densities and (c) The corresponding specific capacitance of AC electrode calculated by the GCD curves.

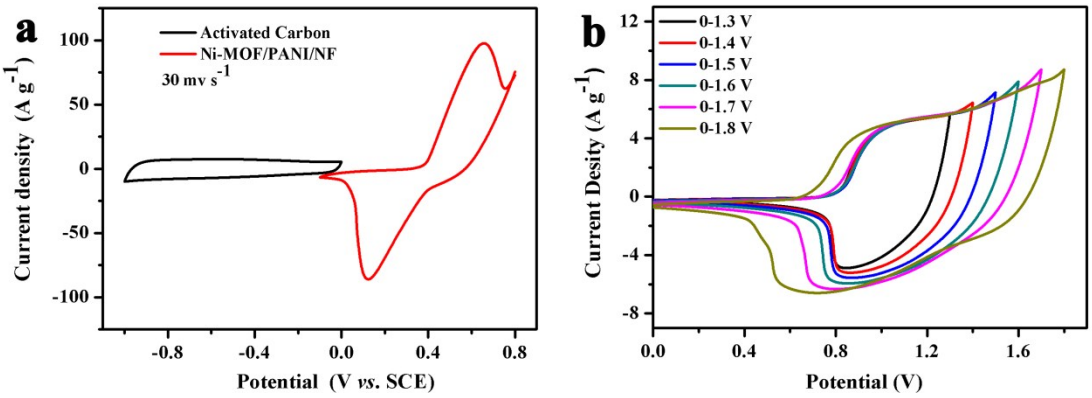

Fig. S9 (a) CV curves of the Ni-MOF/PANI/NF and AC electrodes tested at a scan rate of 30 mV s^{-1} in a three-electrode cell. (b) CV curves of ASC device at different voltage windows with scan rate of 50 mV s^{-1}.

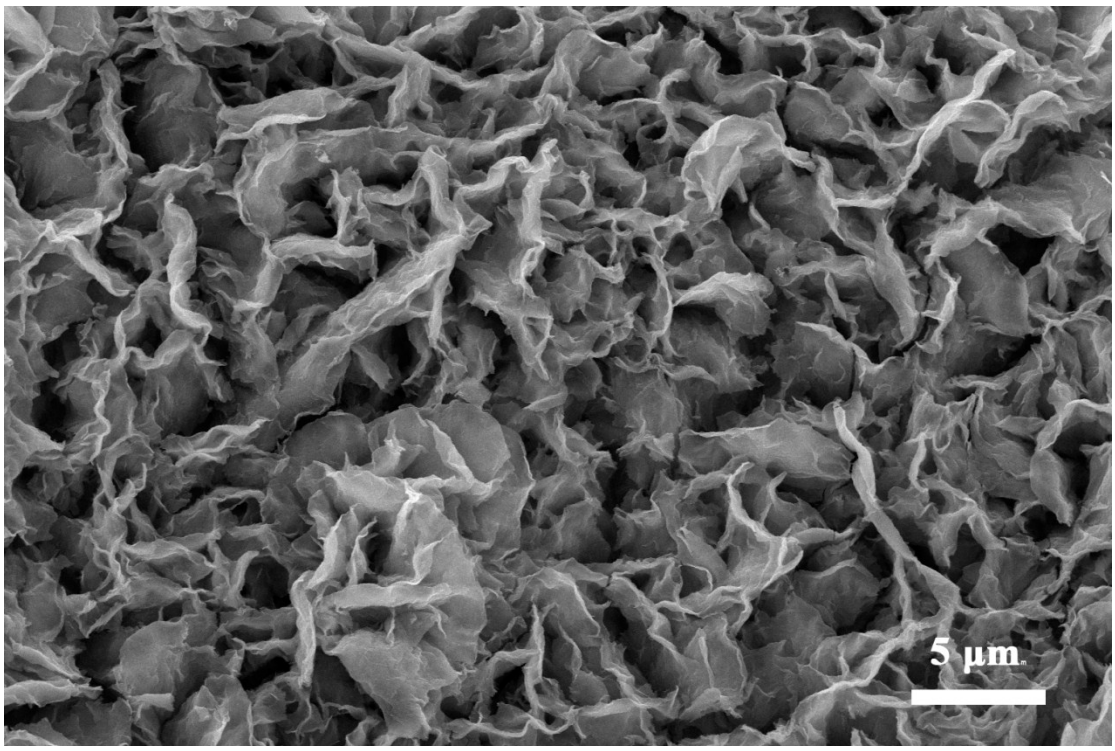

Fig. S10 SEM image of Ni-MOF/PANI/NF after cycling.

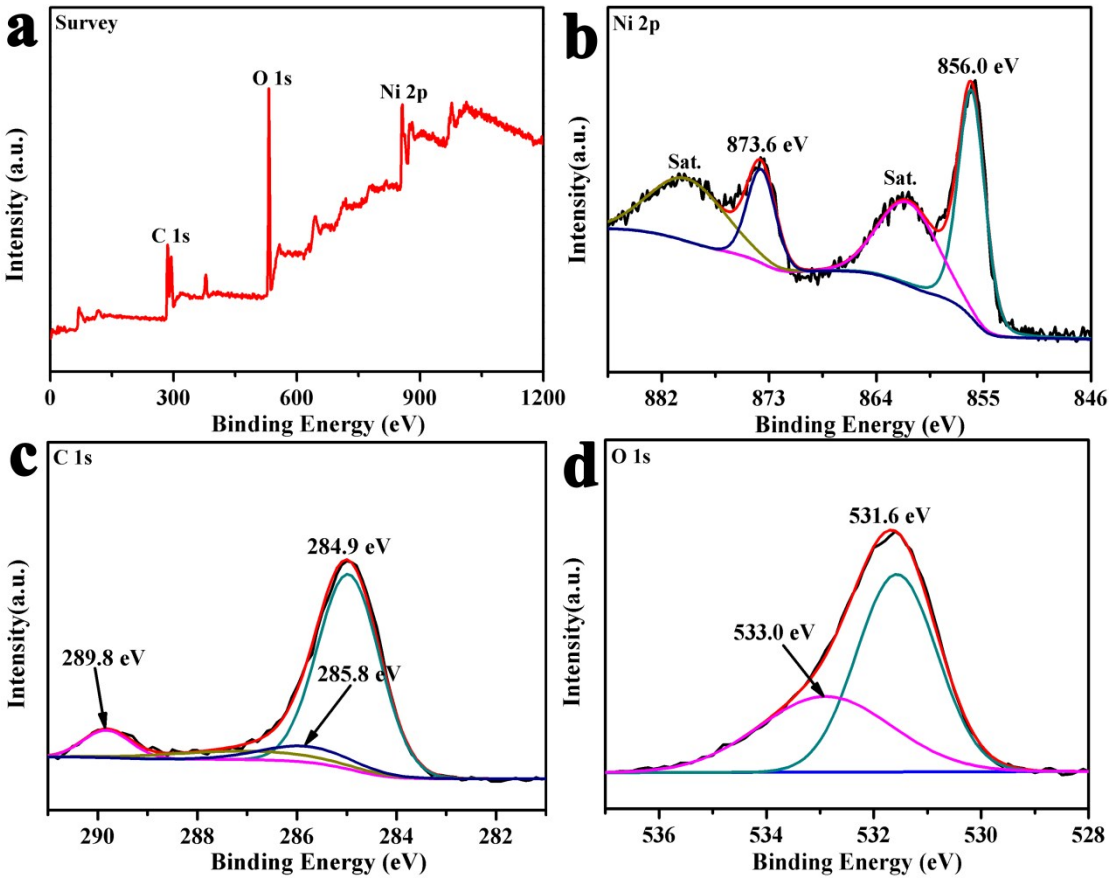

Fig.S11 (a) XPS survey spectrum of Ni-MOF/PANI/NF after cycling. (b-d) High-resolution XPS spectra for Ni, C and O.

Table S1 Electrochemical performance comparison with previous studies.

ASC	Energy density (Wh kg^{-1})	Power density (W kg^{-1})	Cycling stability	Refs
Ni-MOF/PANI//AC	45.6	850.0	81.6%, 10000 cycles	This work
	19.1	8500.0		This work
Co-Mn-MOF//AC	30	2285.7	80%, 3000 cycles	S1
Ni-MOF//AC	31.5	800	50%, 5000 cycles	S2
Hierarchically porous Ni-MOF//AC	21.1	440.0	70.0%, 2000 cycles	S3
2D Ni-MOF//AC	10	1450	97%, 1200 cycles	S4
Cu–CAT NWAs//AC	2.6	200.0	85.%, 5000 cycles	S5
Ni–Tp/PANI	19.9	430.6	82.6, 5000 cycles	S6

References

[S1] S. H. Kazemi, B. Hosseinzadeh, H. Kazemi, M. A. Kiani and S. Hajati, ACS Appl. Mater. Interfaces, 2018, 10, 23063-23073.

[S2] S. Gao, Y. Sui, F. Wei, J. Qi, Q. Meng and Y. He, J. Mater. Sci., 2018, 53, 6807-6818.

[S3] P. Du, Y. Dong, C. Liu, W. Wei, D. Liu and P. Liu, J. Coll. Interface Sci., 2018, 518, 57-68. [4] S. Liu, C. Mao, Y. Niu, F. Yi, J. Hou, S. Lu, J. Jiang, M. Xu, C. Li, ACS Appl. Mater. Interfaces, 2015, 7, 25568–25573.

[S4] T. Deng, W. Zhang, O. Arcelus, D. Wang, X. Shi, X. Zhang, J. Carrasco, T. Rojo and W. Zheng, Comm. Chem., 2018, 1, 6.

[S5] W. Li, K. Ding, H. Tian, M. Yaoui, B. Nath, W. Deng, Y. Wang, X. Gang, Adv. Funct. Mater., 2017, 27, 1702067.

[S6] Q. Chen, S. Lei, P. Deng, X. Ou, L. Chen, W. Wang, Y. Xiao, B. Cheng, J. Mater. Chem. A, 2017, 5, 19323.